Quenching of Molecular Fluorescence on the Surface of Monolayer-Protected Gold Nanoparticles Investigated Using Place Exchange Equilibria

ARTICLE *in* LANGMUIR · MAY 2007

Impact Factor: 4.46 · DOI: 10.1021/la070005a · Source: PubMed

Quenching of Molecular Fluorescence on the Surface of Monolayer-Protected Gold Nanoparticles Investigated Using Place Exchange Equilibria

Nicolas Nerambourg, Martinus H.V. Werts,* Marina Charlot, and Mireille Blanchard-Desce

Synthèse et Electrosynthèse Organiques (UMR6510), CNRS, Université de Rennes 1, Campus de Beaulieu, Bât. 10A, F-35042 Rennes Cedex, France

Received January 2, 2007. In Final Form: February 22, 2007

The insertion of fluorescently labeled thiols into the protecting self-assembled monolayer on the surface of gold nanoparticles through place exchange reactions and the effects of this insertion on the photophysical properties of the fluorophores are investigated. Analysis of solution-phase fluorescence data using a dynamic equilibrium model yields the equilibrium constant for the place exchange equilibrium, as well as the relative fluorescence brightness of the fluorophores on the particle surface. In all cases we find a significant quenching of the fluorescence, and potential reasons for this quenching are discussed. In the case of these relatively small particles (4.5 nm diameter), the quenching appears to be mainly related to enhanced nonradiative deactivation pathways. The place exchange equilibrium constant reveals a reduced affinity of the fluorescently labeled thiols for insertion into the nonfluorescent alkylthiol monolayer ($K_{eq} \approx 0.2$) compared to unlabeled alkylthiols.

1. Introduction

The supramolecular organization of functional molecular modules as ligands on the surface of soluble monolayer-protected noble metal clusters (MPCs) [1] is a promising "supramodular" strategy for the fabrication of nanoscale devices with potential applications in clinical diagnostics, etc.[2−4] The introduction of fluorescent chromophores into the protecting ligand shells around MPCs might turn such clusters into photoluminescent entities that can be traced using fluorescence microscopy or that can act as luminescent probes. The noble metal core of MPCs is rich in conduction electrons that possess collective excitations giving rise to so-called plasmon resonances in the visible part of the electromagnetic spectrum. For the successful construction of chromophore-modified MPCs, it is important to know the effects of these plasmon resonances on the photophysics of nearby chromophores, in particular with respect to their fluorescence.

The effects of metal nanostructures on the photophysics of nearby chromophores and inorganic emitters (e.g., semiconductor quantum dots) are currently receiving increasing attention. The effects are being investigated using different strategies, e.g., through investigations of the luminescence of single quantum dots [5,6] or chromophores [7] near a metal nanostructure, enhancement of Raman scattering,[8] continuum generation,[9] and photochemistry[10] near single lithographically defined metal nanostructures, emitters deposited on top of metal structures, metal nanoparticles coated with fluorescent silica[11] or polymer layers,[12] and fluorescently labeled MPCs.[13−27] MPCs provide a flexible platform for such studies. In this paper we exploit the controlled ligand exchange for the investigation of the quenching of the fluorescence of organic chromophores by a metal nanocore.

In the majority of studies on chromophore-modified MPCs in solution, an efficient quenching of the fluorescence of the chemisorbed chromophores has been observed.[13−27] This quenching is generally ascribed to an increased nonradiative relaxation of the excited state due to energy and/or electron transfer. More detailed studies reveal that the quenching may be partly due to a decrease in the rate of radiative relaxation related to changes in the photonic mode density near the metal cluster surface, a genuine "plasmonic" effect,[27] although studies on very small gold nanoparticles (1.5 nm diameter) do not find indications for such an effect.[28]

* To whom correspondence should be addressed. E-mail: martinus.werts@univ-rennes1.fr.

(1) Templeton, A. C.; Wuelfing, W. P.; Murray, R. W. *Acc. Chem. Res.* **2000**, *33*, 27−36.
(2) Rosi, N. L.; Mirkin, C. A. *Chem. Rev.* **2005**, *105*, 1547−1562.
(3) Shenhar, R.; Rotello, V. M. *Acc. Chem. Res.* **2003**, *36*, 549−561.
(4) Daniel, M. C.; Astruc, D. *Chem. Rev.* **2004**, *104*, 293−346.
(5) Gueroui, Z.; Libchaber, A. *Phys. Rev. Lett.* **2004**, *93*, 166108.
(6) Farahani, J. N.; Pohl, D. W.; Eisler, H. J.; Hecht, B. *Phys. Rev. Lett.* **2005**, *95*, 017402.
(7) Anger, P.; Bharadwaj, P.; Novotny, L. *Phys. Rev. Lett.* **2006**, *96*, 113002.
(8) Fromm, D. P.; Sundaramurthy, A.; Kinkhabwala, A.; Schuck, P. J.; Kino, G. S.; Moerner, W. E. *J. Chem. Phys.* **2006**, *124*, 061101.
(9) Mühlschlegel, P.; Eisler, H. J.; Martin, O. J. F.; Hecht, B.; Pohl, D. W. *Science* **2005**, *308*, 1607−1609.
(10) Sundaramurthy, A.; Schuck, P. J.; Conley, N. R.; Fromm, D. P.; Kino, G. S.; Moerner, W. E. *Nano Lett.* **2006**, *6*, 360.
(11) Tovmachenko, O. G.; Graf, C.; Van den Heuvel, D. J.; Van Blaaderen, A.; Gerritsen, H. C. *Adv. Mater.* **2006**, *18*, 91−95.
(12) Schneider, G.; Decher, G.; Nerambourg, N.; Praho, R.; Werts, M. H. V.; Blanchard-Desce, M. *Nano Lett.* **2006**, *6*, 530−536.
(13) Templeton, A. C.; Cliffel, D. E.; Murray, R. W. *J. Am. Chem. Soc.* **1999**, *121*, 7081−7089.
(14) Aguila, A.; Murray, R. W. *Langmuir* **2000**, *16*, 5949−5954.
(15) Hu, J.; Zhang, J.; Liu, F.; Kittredge, K.; Whitesell, J. K.; Fox, M. A. *J. Am. Chem. Soc.* **2001**, *123*, 1464−1470.
(16) Zhang, J.; Whitesell, J. K.; Fox, M. A. *Chem. Mater.* **2001**, *13*, 2323−2331.
(17) Ipe, B. I.; Thomas, K. G.; Barazzouk, S.; Hotchandani, S.; Kamat, P. V. *J. Phys. Chem. B* **2002**, *106*, 18−21.
(18) Sudeep, P. K.; Ipe, B. I.; Thomas, K. G.; George, M. V.; Barazzouk, S.; Hotchandani, S.; Kamat, P. V. *Nano Lett.* **2002**, *2*, 29−35.
(19) Huang, T.; Murray, R. W. *Langmuir* **2002**, *18*, 7077−7081.
(20) Gu, T.; Whitesell, J. K.; Fox, M. A. *Chem. Mater.* **2003**, *15*, 1358−1366.
(21) Zhang, J.; Whitesell, J. K.; Fox, M. A. *J. Phys. Chem. B* **2003**, *107*, 6051−6055.
(22) Montalti, M.; Prodi, L.; Zaccheroni, N.; Baxter, R.; Teobaldi, G.; Zerbetto, F. *Langmuir* **2003**, *19*, 5172−5174.
(23) Fan, C.; Wang, S.; Hong, J. W.; Bazan, G. C.; Plaxco, K. W.; Heeger, A. J. *Proc. Natl. Acad. Sci. U.S.A.* **2003**, *100*, 627.
(24) Werts, M. H. V.; Zaim, H.; Blanchard-Desce, M. *Photochem. Photobiol. Sci.* **2004**, *3*, 29−32.
(25) Montalti, M.; Prodi, L.; Zaccheroni, N.; Battistini, G. *Langmuir* **2004**, *20*, 7884−7886.
(26) Ghosh, S. K.; Pal, A.; Kundu, S.; Nath, S.; Pal, T. *Chem. Phys. Lett.* **2004**, *395*, 366−375.
(27) Dulkeith, E.; Ringler, M.; Klar, T. A.; Feldmann, J.; Javier, A. M.; Parak, W. J. *Nano Lett.* **2005**, *5*, 585.

10.1021/la070005a CCC: $37.00
Published on Web 03/31/2007

Enhancement of fluorescence by metal nanostructures has been reported as well, mostly in aggregated metal colloids.[29,30] The enhancement effects appear particularly pronounced with precipitates of metal colloid aggregates on surfaces.[31] These effects are closely related to the enhancement observed in surface-enhanced Raman scattering (SERS).[32] The particle aggregates have random nanoscale geometries that contain fortuitous photonic "hot spots",[33] where the electromagnetic radiation field is intensified through localized plasmon resonances. It is a current challenge to rationally design and construct such "photonic hot spots". Studies of well-defined self-assembled systems such as chromophore-modified MPCs may provide the bricks and the basic knowledge toward the rational assembly of such fluorescence enhancing hot spots.

Molecular fluorescence is characterized by the competition of radiative and nonradiative deactivation channels of an excited chromophore, each described by a monomolecular reaction rate constant (k_f and k_{nr}, respectively):

$$F^* \xrightarrow{k_f} F + h\nu$$

$$F^* \xrightarrow{k_{nr}} F + \text{heat}$$

The rates of k_f and k_{nr} can be deduced from measurements of the fluorescence quantum yield, Φ_f, and the observed fluorescence decay time, τ_{obs}. In most cases, changes in the fluorescence quantum yield of a given chromophore are only due to changes in the nonradiative rate, k_{nr}, which may for example receive contributions from energy or electron-transfer processes. The radiative rate k_f remains more or less constant. On the surface of metal structures such as MPCs, however, k_f may profoundly change. Experimental evidence for changes in k_f near gold nanoparticles in suspension has been found recently.[12,27] All of the particles used in those studies were of sufficient size (diameter > 4 nm) to display the well-known surface plasmon polariton (SPP) absorption band. In contrast, in chromophore−particle assemblies based on very small 1.5 nm diameter gold nanoparticles (in which the SPP band is absent), no decrease of k_f was found, and the observed quenching of fluorescence could be attributed by contributions to nonradiative deactivation only.[28] Further experimental studies will help the development and refinement of theoretical descriptions [34−36] of molecular photophysics near metal surfaces.

The present work aims to obtain additional experimental information on the effects of metal cluster cores on the radiative and nonradiative deactivation of molecular fluorophores by making use of thiol exchange chemistry on the surface of gold nanoparticles. Three different chromophores have been modified to carry an alkylthiol chain which enables them to be inserted into the protecting monolayer at the surface of MPCs through ligand exchange reactions (Figure 1). In ligand exchange at the surface of MPCs,[37−39] an incoming thiol inserts itself into the monolayer on the surface of the metal cluster, expelling another thiol. This allows us to analyze the changes in the optical absorption and emission of the chromophores as a result of binding of the chromophores to the MPCs and to assess to what extent the fluorescence is quenched and how much of it can be retained for practical applications. Of the three chromophores studied in this work, pyrene has been studied previously in conjunction with gold MPCs, and all studies reported a quenching of its fluorescence.[17,22,25,40,41] The quenching of a chromophore by MPCs may differ depending on the chromophore. Therefore, we have chosen to include different chromophores in this study: an asymmetric push−pull chromophore (dialkylaminonitrostilbene derivative, DANS) and a symmetrical push−pull−push chromophore (bis(dialkylaminophenylene)biphenyl derivative, DABP) to investigate the influence of the chromophore structure on the nanoparticle-induced fluorescence quenching (Figure 1). The DABP chromophore has the additional characteristic of displaying a large two-photon absorption cross section,[42] which will enable future investigations of the effect of metal nanoparticles on two-photon excited fluorescence. The present work will be concerned with monophotonic absorption and fluorescence.

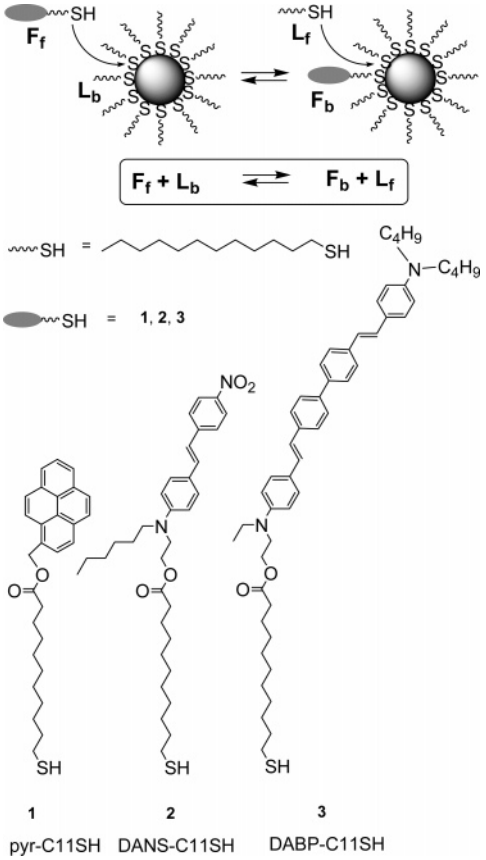

Figure 1. Attachment of fluorescent chromophores to gold nanoparticles through ligand exchange using thiol-modified chromophores.

(28) Jennings, T. L.; Singh, M. P.; Strouse, G. F. *J. Am. Chem. Soc.* **2006**, *128*, 5462−5467.
(29) Gryczynski, I.; Malicka, J.; Holder, E.; DiCesare, N.; Lakowicz, J. R. *Chem. Phys. Lett.* **2003**, *372*, 409−414.
(30) Nabika, H.; Deki, S. *J. Phys. Chem. B* **2003**, *107*, 9161−9164.
(31) Wenseleers, W.; Stellacci, F.; Meyer-Friedrichsen, T.; Mangel, T.; Bauer, C. A.; Pond, S. J. K.; Marder, S. R.; Perry, J. W. *J. Phys. Chem. B* **2002**, *106*, 6853−6863.
(32) Campion, A.; Kambhampati, P. *Chem. Soc. Rev.* **1998**, *27*, 241−250.
(33) Michaels, A. M.; Jiang, J.; Brus, L. *J. Phys. Chem. B* **2000**, *104*, 11965−11971.
(34) Carminati, R.; Greffet, J. J.; Henkel, C.; Vigoureux, J. M. *Opt. Comm.* **2006**, *261*, 375.
(35) Andreussi, O.; Corni, S.; Mennucci, B.; Tomasi, J. *J. Chem. Phys.* **2004**, *121*, 10190−10202.
(36) Gersten, J.; Nitzan, A. *J. Chem. Phys.* **1981**, *75*, 1139−1152.
(37) Hostetler, M.; Green, S.; Stokes, J. J.; Murray, R. W. *J. Am. Chem. Soc.* **1996**, *118*, 4212−4213.
(38) Hostetler, M. J.; Templeton, A. C.; Murray, R. W. *Langmuir* **1999**, *15*, 3782−3789.
(39) Ingram, R. S.; Hostetler, M. J.; Templeton, A. C.; Murray, R. W. *J. Am. Chem. Soc.* **1997**, *119*, 9175−9178.
(40) Ipe, B. I.; Thomas, K. G. *J. Phys. Chem. B* **2004**, *108*, 13265−13272.
(41) Werts, M. H. V.; Zaim, H.; Blanchard-Desce, M. *Photochem. Photobiol. Sci.* **2004**, *3*, 29−32.
(42) Mongin, O.; Porrès, L.; Charlot, M.; Katan, C.; Blanchard-Desce, M. *Chem. Eur. J.* **2007**, *13*, 1481−1498.

2. Ligand Exchange Equilibrium Model

Ligand exchange at the surface of gold nanoparticles is a well-established method for attaching functional molecular modules to these particles. The exchange proceeds through an associative ("S_N2-like") mechanism in which an incoming thiol ligand expulses an existing ligand.[1,38] Since the liberated thiol in turn can replace another thiol on the surface, a dynamic equilibrium is created when free thiols are added to a solution of MPCs. An equilibrium constant, K, is associated with this equilibrium. Very recently, this type of equilibrium has been studied in detail for pairs of chemically very similar linear alkylthiols using gas chromatography, obtaining equilibrium constants close to unity.[43] In the present paper we develop a simple model of the equilibrium of ligand exchange reactions at the surface of MPCs that enables us to analyze and interpret the fluorimetric studies on ligand exchange and to obtain both the equilibrium constant of the ligand exchange for the pairs of thiols used and the relative fluorescence brightness of a bound fluorophore compared to that of a free fluorophore.

When free thiol-modified fluorophores (designated F_f) are introduced in a solution of dodecanethiol/gold MPCs, they can penetrate the protecting monolayer of bound dodecanethiols (denoted L_b), binding themselves to the gold (and thus becoming bound fluorophore F_b) and liberating a nonfluorescent thiol (denoted L_f), according to

$$F_f + L_b \rightarrow F_b + L_f \tag{1}$$

Conversely, the liberated nonfluorescent thiols, L_f, can re-enter the monolayer and replace bound fluorophores (eq 2).

$$L_f + F_b \rightarrow L_b + F_f \tag{2}$$

When there are more thiols present in the solution than thiol binding sites (i.e., all thiol binding sites are occupied), the labeled and unlabeled thiols are competing for binding sites on the MPC surface, establishing a dynamic equilibrium that can be described by eqs 3 and 4.

$$L_f + F_b \overset{K}{\rightleftharpoons} L_b + F_f \tag{3}$$

$$K = \frac{[L_f][F_b]}{[L_b][F_f]} \tag{4}$$

We start each place exchange experiment with a solution of purified gold MPCs protected by a monolayer of *n*-dodecanethiol. In this solution the concentration of *n*-dodecanethiol is equal to the concentration of binding sites (c_{sites}) since all binding sites are occupied by dodecanethiol and no free thiols are present, nor any fluorescently labeled thiol. The thiol composition of this solution is given by

$$[L_b] = c_{sites} \quad \text{and } [L_f] = [F_f] = [L_b] = 0 \tag{5}$$

The concentrations of L_f, F_b, L_b, and F_f are normalized using the total concentration of thiol binding sites (c_{sites}) so that all concentrations are expressed as fractions of the total concentration of thiol binding sites (eq 6).

$$L_f = \frac{[L_f]}{c_{sites}}, \quad F_f = \frac{[F_f]}{c_{sites}}, \quad L_b = \frac{[L_b]}{c_{sites}}, \quad \text{and } F_b = \frac{[F_b]}{c_{sites}} \tag{6}$$

The thiol composition of the initial solution containing only *n*-dodecanethiol gold MPCs is thus expressed as in eq 7.

$$L_b = 1 \quad \text{and } L_f = F_f = F_b = 0 \tag{7}$$

Subsequently, a known concentration of free thiol-modified fluorophores ($c_{fluorophores}$) is added to the solution. As with the other thiol concentrations, this concentration can be expressed as the fraction of the concentration of ligand binding sites, referred to as β (eq 8).

$$\beta = \frac{c_{fluorophores}}{c_{sites}} \tag{8}$$

After the addition, an excess of thiols is present and a competition for binding sites on the particle surface will start, with thiols continuously inserting themselves in the particle monolayer and expelling another thiol. The solution will evolve to arrive at a new equilibrium. The goal is to calculate L_f, F_f, L_b, and F_b (and thus $[L_f]$, $[F_f]$, $[L_b]$, and $[L_f]$) from K and β once the new equilibrium has been reached. The mass balance of the system is expressed in eq 9a−d.

$$L_f + L_b = 1 \tag{9a}$$

$$F_f + F_b = \beta \tag{9b}$$

$$L_f + F_f = \beta \tag{9c}$$

$$L_b + F_b = 1 \tag{9d}$$

Since the other concentrations can be readily deduced once one concentration is known, it is only necessary to find an expression for only one concentration, e.g., F_f. Expressing eq 4 with the aid of the relations in eq 9a−d leads to eq 10.

$$K = \frac{\beta^2 - 2\beta F_f + F_f^2}{F_f - \beta F_f + F_f^2} \tag{10}$$

In the special case that $K = 1$, we find the solutions expressed in eq 11.

$$F_f = \frac{\beta^2}{\beta + 1}, \quad F_b = \frac{\beta}{\beta + 1}, \quad L_f = \frac{\beta}{\beta + 1}, \quad L_b = \frac{1}{\beta + 1} \tag{11}$$

Also for $K \neq 1$, a solution exists. The concentration of free thiol-modified fluorophores (F_f) can be found using eq 12. The concentrations of the other species are then found using the relations of eq 9.

$$F_f = \frac{-b - \sqrt{b^2 - 4ac}}{2a} \tag{12}$$

with

$$a = 1 - K$$

$$b = \beta(K - 2) - K$$

$$c = \beta^2$$

Knowing the relative concentrations of all thiols, the fluorimetric behavior of the solution can be described. The observed total (integrated) fluorescence emission intensity, I, is only due to the contributions from free and bound fluorophores, F_f and F_b, but not from the other ligand (typically, *n*-dodecanethiol)

(43) Kassam, A.; Bremner, G.; Clark, B.; Ulibarri, G.; Lennox, B. R. *J. Am. Chem. Soc.* **2006**, *128*, 3476−3477.

since this other ligand (present as bound L_b and free L_f) is not fluorescent under the experimental conditions used (eq 13).

$$I = I_{free} + I_{bound} \propto F_f \epsilon_{Ff} \Phi_{Ff} + F_b \epsilon_{Fb} \Phi_{Fb} \qquad (13)$$

where ϵ_{Ff} and ϵ_{Fb} are the extinction coefficients at the excitation wavelength of free and bound thiol-modified fluorophores, respectively, and Φ_{Ff} and Φ_{Fb} are the corresponding fluorescence quantum yields.

For our experiments it is convenient to measure the ratio of the total fluorescence intensity of thiol-modified fluorophores in the presence of MPCs and the fluorescence intensity of the same concentration of fluorophores in the absence of MPCs (I_0), as this ratio is independent of instrument settings, and simplifies the analysis. It is found that the ratio (I/I_0) can be expressed as in eq 14.

$$I/I_0 = \frac{1}{\beta}(F_f + F_b Q) \qquad (14)$$

The factor Q represents the brightness of a bound fluorophore, $\epsilon_{Fb}\Phi_{Fb}$, relative to the brightness of the free fluorophore, $\epsilon_{Ff}\Phi_{Ff}$:

$$Q = \frac{\epsilon_{Fb}\Phi_{Fb}}{\epsilon_{Ff}\Phi_{Ff}} \qquad (15)$$

We note that in eq 14, F_f and F_b are both functions of β and K. The factor Q and equilibrium constant K can be obtained by measurements of the relative fluorescence intensities (I/I_0) of equilibrated solutions of MPCs in the presence of varying quantities of added thiol-modified fluorophores (varying β) and fitting of eq 14 to the results.

The model presented here is simple and does not take into account the existence of different types of binding sites that may be present at the surface of MPCs. These different binding sites may each have different kinetics of exchange and equilibrium constants. The equilibrium constant used in the model is therefore an "average" binding constant. Additionally, the model implicitly assumes that the number of accessible thiol binding sites is independent from the nature of the ligand. As long as the alkylthiol linker of the incoming fluorescent thiol is structurally similar to the alkylthiols in the initial monolayer and the amount of incoming thiol remains low, this assumption probably holds. Deviations from this assumption will translate into a change of the observed binding constant.

In spite of these simplifications, however, the model allows for a distinction between chromophores that are free in solution and those that are bound to an MPC. The fluorescence of the chromophores that are free in solution are not influenced by the MPCs at the concentrations used (cf. the Results section and Figure 3), whereas the bound chromophores do experience the effect of the MPC gold core, which can be quantitatively assessed. It will be shown that the fluorimetric titration curves can be reliably reproduced using the presented model, yielding both the equilibrium constant, K, and the relative fluorescence intensity, Q, of a bound chromophore compared to that of a free chromophore.

3. Experimental Section

3.1. Synthesis of Thiol-Modified Chromophores. Solvents were generally dried and distilled prior to use. Reactions were monitored by thin-layer chromatography on Merck silica gel 60 F_{254} precoated aluminum sheets. Column chromatography: Merck silica gel Si 60 (40−63 μm, 230−400 mesh). NMR: ^{1}H chemical shifts (δ) are given in ppm relative to TMS as internal standard, J values in Hz, ^{13}C chemical shifts relative to the central peak of $CDCl_3$ at 77.0 ppm. High-resolution mass spectra measurements were performed at the Centre Régional de Mesures Physiques de l'Ouest (C.R.M.P.O., Rennes), using a Micromass MS/MS ZABSpec TOF instrument with EBE TOF geometry; LSIMS (liquid secondary ion mass spectrometry) at 8 kV with Cs^+ in *m*-nitrobenzyl alcohol (mNBA); ES+ (electrospray ionization, positive mode) at 4 kV; EI (electron ionization) at 70 eV.

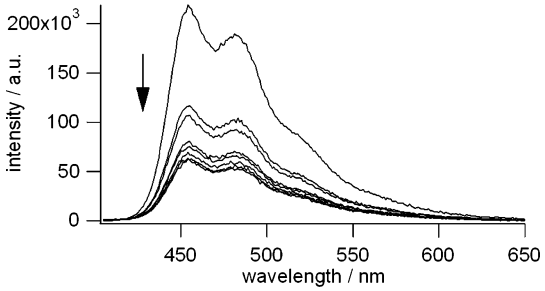

Figure 2. Time-evolution of the emission spectrum (λ_{exc} = 398 nm) of dye **3** DABP-C11SH (1.28×10^{-5} M, 2% with respect to the concentration of binding sites, $\beta = 0.02$) upon addition to 4.5 nm diameter gold MPCs (1.63×10^{-6} M in particles) in air-equilibrated toluene. Each spectrum corresponds to a 100× diluted sample from the reaction mixture. The first spectrum is the free dye. Subsequent spectra have been taken after, respectively, 2.25, 3.83, 19.7, 26.4, 43.6, 71.9, and 140 h. The spectra have been corrected for detection sensitivity and residual inner filter effects (see Experimental Section).

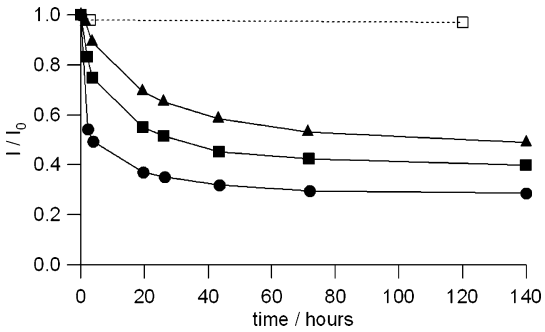

Figure 3. Time-evolution of the relative fluorescence intensity (I/I_0) of DABP-C11SH in air-equilibrated toluene (λ_{exc} = 398 nm) during ligand exchange with *n*-dodecanethiol protected gold nanoparticles for different amounts of incoming DABP-C11SH: β = 0.10 (▲), 0.05 (■), and 0.02 (●). The open squares represent the intensities for DABP (the dye without the alkylthiol chain) in the presence of gold MPCs, showing that at the concentration used there is no interaction between non-thiolated dye and nanoparticles.

Alkylthiol-modified chromophores were prepared by esterification of alcohol-bearing dyes with 11-mercaptoundecanoic acid. Under the conditions used, no protecting group on the thiol was needed and formation of disulfides was not observed.

*Pyr-C11SH (**1**).* Dicyclohexyl carbodiimide (DCC, 190 mg, 0.921 mmol) was added to a solution of 11-mercaptoundecanoic acid (200 mg, 0.915 mmol), 1-pyrene methanol (210 mg, 0.915 mmol), and DMAP (*p*-(dimethylamino)pyridine, 9 mg, 0.073 mmol) in ethanol-free CH_2Cl_2 at room temperature. The mixture was stirred overnight under argon, and the solvent was removed under reduced pressure. Thereafter, the crude product was purified by column chromatography (heptane/CH_2Cl_2 50:50) to yield 190 mg (50%) of **1**. ^{1}H NMR (300.13 MHz, $CDCl_3$) δ 8.30−8 (m, 9H), 5.85 (s, 2H), 2.50 (q, J = 7.3, 2H), 2.40 (t, J = 7.4, 2H), 1.67 (t, J = 7.3, 2H), 1.57 (quint, J = 7.4, 2H), 1.37−1.19 (m, 12H); ^{13}C NMR (75.47 MHz, $CDCl_3$) δ 173.83, 131.68, 131.18, 130.67, 129.5, 129.04, 128.12, 127.78, 127.76, 127.35, 126.06, 125.48, 125.40, 124.86, 124.63, 124.59, 122.94, 64.55, 34.39, 34.00, 29.34, 29.29, 29.16, 29.05, 28.96, 28.30, 24.98, 24.62; HRMS (EI) calcd for $C_{28}H_{32}O_2S$ ($M^{+\bullet}$) m/z 432.21230, found 432.2108. Anal. Calcd for $C_{28}H_{32}O_2S$: C, 77.74; H, 7.46; S, 7.41. Found: C, 77.77; H, 7.51; S, 7.34.

DANS-C11SH (2). DCC (77.4 mg, 0.375 mmol) was added to a solution of 11-mercaptoundecanoic acid (65.5 mg, 0.300 mmol), 2-[hexyl{4-[(1E)-2-(4-nitrophenyl)-ethenyl]phenyl}amino]-ethanol [44] (92.2 mg, 0.250 mmol), and DMAP (3 mg, 0.024 mmol) in CH_2Cl_2 stabilized with amylene at room temperature. The mixture was stirred for 3 h under argon and the solvent was removed under reduced pressure. Thereafter, the crude product was purified by column chromatography (heptane/CH_2Cl_2 40:60) to yield 142 mg (41%) of **2**. ^{1}H NMR (200.13 MHz, $CDCl_3$) δ 8.21 and 7.58 (AA'XX', $J_{AX} = 8.7$, 4H), 7.45 and 6.74 (AA'XX', $J_{AX} = 9.1$, 4H), 7.23 (d, $J = 16.2$, 1H), 6.93 (d, $J = 16.2$, 1H), 4.28 (t, $J = 6.3$, 2H), 3.64 (t, $J = 6.3$, 2H), 3.64 (t, $J = 7.6$, 2H), 2.54 (q, $J = 7.3$, 2H), 2.33 (t, $J = 7.5$, 2H), 1.65−1.56 (m, 4H), 1.40−1.30 (m, 20H), 0.94 (t, $J = 6$, 3H); ^{13}C NMR (75.47 MHz, $CDCl_3$) δ 173.77, 148.38, 145.86, 145.00, 133.53, 128.63, 126.05, 124.15, 121.46, 111.85, 61.17, 51.31, 49.22, 34.23, 34.01, 31.70, 29.44, 29.37, 29.24, 29.12, 29.05, 28.35, 27.13, 26.73, 24.87, 24.64, 22.68, 14.05; HRMS (ES^+) calcd for $C_{33}H_{48}N_2O_4NaS$ ($[M + Na]^+$) *m*/*z* 591.32325, found 591.3249.

DABP-C11SH (3). For the synthesis of **3** a hydroxy-terminated derivative of DABP was used, of which the synthesis is described in the Supporting Information. DCC (4.85 mg, 0.023 mmol) was added to a solution of 11-mercaptoundecanoic acid (5.13 mg, 0.023 mmol), hydroxy-terminated DAPB derivative 2-[[4-[(1*E*)2-[1,1′-[(1*E*)-2-[4-(dibutylamino)phenyl]ethenyl]biphenyl]ethenyl]phenyl]-ethylamino]ethanol (13.45 mg, 0.021 mmol), and DMAP (1.23 mg, 0.01 mmol) in 2 mL of CH_2Cl_2 stabilized with amylene at room temperature. The mixture was stirred for 3 h under argon and the solvent was removed under reduced pressure. Thereafter, the crude product was purified by column chromatography (heptane/CH_2Cl_2 50:50) to yield 13.6 mg (52%) of **3**. ^{1}H NMR (300.13 MHz, $CDCl_3$) δ 7.59 et 7.52 (AA'XX', $J_{AX} = 8.5$, 8H), 7.41 et 7.39 (AA'XX', $J_{AX} = 8.8$, 4H), 7.08 (AB, $J_{AB} = 16.30$, 2H), 6.92 (AB, $J_{AB} = 16.30$, 1H), 6.90 (AB, $J_{AB} = 16.30$, 1H), 6.71 et 6.63 (AA'XX', $J_{AX} = 8.8$, 4H), 4.24 (t, $J = 6.30$, 2H), 3.57 (t, $J = 6.30$, 2H), 3.43 (q, $J = 6.96$, 2H), 3.29 (t, $J = 7.40$, 4H), 2.50 (q, $J = 7.33$, 2H), 2.29 (t, $J = 7.40$, 2H), 1.57 (m, 4H), 1.27 (m, 20H), 1.19 (t, $J = 6.96$, 3H), 0.96 (t, $J = 7.10$, 6H). HRMS (ES^+) calcd for $C_{51}H_{69}N_2O_2S^+$ ($[M + H]^+$) *m*/*z* 773.50798, found 773.5082.

3.2. Preparation of *n*-Dodecanethiol-Protected Gold Nanoparticles. *n*-Dodecanethiol-stabilized gold nanoparticles of 4.5 nm diameter were prepared according to a slightly modified literature procedure.[45] A 25 mL aqueous solution of $HAuCl_4 \cdot 3H_2O$ (0.35 g, 0.88 mmol) was added to a solution of tetraoctylammonium bromide (1.51 g, 2.76 mmol) in toluene (80 mL). The mixture was stirred until the tetrachloroaurate was transferred into the organic phase (the aqueous phase became progressively colorless and the organic phase became deeply red). The two phases were separated, and 25 mL of a fresh aqueous solution of $NaBH_4$ (0.38 g, 10 mmol) was added slowly under vigorous stirring to reduce the $AuCl_4^-$. The organic phase became dark red. After 2.5 h of stirring, the two phases were separated and the organic phase was successively washed with 0.1 M HCl (30 mL), a saturated solution of $NaHCO_3$ (30 mL), and brine (30 mL). The organic phase was dried over Na_2SO_4 and filtered. *n*-Dodecanethiol (0.180 g 0.88 mmol) was added and the mixture was stirring during 48 h to obtain MPCs. The MPC solution was evaporated roughly to 10 mL. Particles were precipitated by addition of isopropyl alcohol and centrifuged to remove the excess of dodecanethiols. The particles were taken up in a minimal quantity of toluene, isopropyl alcohol was added, and the precipitated particles collected by centrifugation. This procedure was repeated four times. Particles were dissolved in toluene and filtered with 200 nm membrane filters (Whatman Anotop 10 Plus) to remove any aggregates and microscopic dust. The gold MPCs were characterized by UV−vis spectroscopy and by transmission electron microscopy (TEM, see Supporting Information). The average core size of the obtained gold MPCs is 4.5 nm.

3.3. Optical Absorption and Emission Spectroscopy. Optical spectroscopy was carried out on air-equilibrated solutions contained in standard 1 cm quartz cuvettes. UV−visible absorption spectra were recorded on a Jasco V-570 instrument. Fluorescence spectra were measured in right-angle configuration using an Edinburgh Instruments FLS920, equipped with a 450 W Osram Xe lamp and a Hamamatsu R928 red-sensitive photomultiplier operating in photon counting mode. The maximum optical density of the samples did not exceed 0.1. In addition to the standard correction for the wavelength dependence of the detection sensitivity, a correction was applied for inner filter effects. These effects may slightly attenuate the excitation intensity and reabsorb emitted photoluminescence and therefore lead to an underestimation of the light intensity in the most strongly absorbing samples. First, the transmission spectrum, *T*, of a given sample is calculated for 0.5 cm path length on basis of the UV−visible absorption spectrum, *A*:

$$T(\lambda) = 10^{-0.5A(\lambda)} \tag{16}$$

The fully corrected emission spectrum, F_{corr}, is then obtained from the uncorrected raw emission spectrum, F_{raw}, using

$$F_{corr}(\lambda_{em}) = k_{corr}(\lambda_{em}) \frac{F_{raw}(\lambda_{em})}{T(\lambda_{exc})T(\lambda_{em})} \tag{17}$$

where k_{corr} is the correction factor for the wavelength dependence of the detection sensitivity, λ_{exc} is the excitation wavelength, and λ_{em} is the emission wavelength. Numerical data treatment was carried out using IGOR Pro software (version 5.03, Wavemetrics, Lake Oswego, OR) running under Windows 2000/XP.

3.4. Determination of the Number of Binding Sites per Particle. The relative amount of incoming chromophore-modified thiols, β (see Section 2), needs to be precisely controlled, and therefore, it is necessary to determine the number of thiol binding sites present in the MPC solutions. From the TEM measurements, the average particle diameter is found to be $d = 4.5$ nm (± 1.1 nm). Data published on a series of monolayer-protected gold nanoparticles of varying size [46] allow us to determine the number of binding sites. Through interpolation of these data it is found that the number of binding sites per MPC can be estimated using $77.9r^2$ and the number of gold atoms per nanoparticle using $283.7r^3$, where *r* is the particle radius (half the diameter, $r = d/2$) expressed in nanometers (see Supporting Information for details). We estimate that the average number of binding sites per particle is 394 (for a total of 3227 gold atoms in the particle). The paper by Hostetler et al. also reports absorption spectra[46] from which an extinction coefficient per particle can be determined, $\epsilon_{particle} = 6.15 \times 10^6$ L mol^{-1} cm^{-1} at 518 nm (2.2 nm radius, 4.4 nm diameter). From the extinction coefficient per particle and the number of binding sites per particle, it is useful to calculate the extinction coefficient per thiol binding site for these particles, since this enables us to relate directly the UV−vis absorption of an MPC solution to the concentration of thiol binding sites. This yields $\epsilon_{site} = 1.56 \times 10^4$ L mol^{-1} cm^{-1}.

Alternatively, ϵ_{site} can also be obtained from previous fluorimetric titration experiments carried out in our group on so-called "naked particles",[41] which is a suspension of gold nanoparticles that do not carry any capping thiols on their surface, but are stabilized by the tetraoctylammonium bromide (TOAB) used in the particle synthesis. These particles are prepared in the same way as the particles in the present study, with the difference that the synthesis is stopped before addition of the *n*-dodecanethiol capping agent. The TOAB-stabilized suspension in toluene contains particles with the same size as the capped MPCs, only without the thiols.

The concentration of binding sites in a naked particle suspension can be deduced from a fluorimetric titration in which aliquots of the naked particle suspension are added to a solution of disulfides of which a small fraction is labeled with fluorescent pyrene chro-

(44) Terenziani, F.; Mongin, O.; Katan, C.; Bhattula, B. K. G.; Blanchard-Desce, M. *Chem. Eur. J.* **2006**, *12*, 3089−3102.

(45) Brust, M.; Walker, M.; Bethell, D.; Schiffrin, D. J.; Whyman, R. J. *Chem. Soc. Chem. Commun.* **1994**, 801−802.

(46) Hostetler, M. J.; Wingate, J. E.; Zhong, C. J.; Harris, J. E.; Vachet, R. W.; Clark, M. R.; Londono, J. D.; Green, S. J.; Stokes, J. J.; Wignall, G. D.; Glish, G. L.; Porter, M. D.; Evans, N. D.; Murray, R. W. *Langmuir* **1998**, *14*, 17−30.

mophores (see Supporting Information). Combined with measurement of the UV−vis spectrum of the same particles capped using an excess of disulfide ligands, our data yield $\epsilon_{site} = 1.34 \times 10^4$ L mol^{-1} cm^{-1}, which is in excellent agreement considering the fundamentally different methods of determination. Interestingly, the literature values[46] for the number of binding sites per particle are derived from modeling based on the known "footprint" for alkylthiol chains in a densely packed monolayer on a gold surface. The agreement with the value that we obtained through titration suggests that the gold particle surface is indeed densely covered with thiols.

3.5. Fluorimetric Study of Ligand Exchange. Ligand exchange is performed on optically concentrated solutions of *n*-dodecanethiol MPCs of known concentrations in thiol binding sites (cf. Section 3.4). Typically, 1.63×10^{-6} M particle solutions are used, corresponding to 6.42×10^{-4} M of thiol binding sites. At $t = 0$, the nonfluorescent alkylthiol MPCs are exposed to a determined concentration of fluorescently tagged alkylthiol, e.g., 6.42×10^{-5} M for $\beta = 0.1$.

For fluorimetric sampling of the equilibration of ligand exchange in time, small aliquots are taken from the exchange solution and diluted 100 times to arrive at optically dilute samples suitable for fluorescence spectroscopy. It was verified that the fluorescence signal of the diluted samples remained stable on time scales between seconds and hours after the dilution to check that the fluorescence intensity of the diluted solution is a proper measure of the behavior of the concentrated solution. The fluorescence measurements were corrected for residual inner filter effects (see Section 3.3).

The decrease in fluorescence intensity accompanying the ligand exchange is monitored over several days until it reaches a constant level corresponding to the equilibrium intensity. All fluorescence intensity (I) measurements are referenced against a solution containing only fluorescently labelled thiols whose intensity is I_0. The samples were excited at the wavelength of the absorption maximum of each chromophore.

4. Results and Discussion

After mixing a stock solution of *n*-dodecanethiol MPCs with solutions of each of the thiol-modified fluorophores, the fluorescence intensity of these solutions decreases and reaches a new constant level after ∼100 h. The evolution of the fluorescence intensity in time is exemplified in Figure 2. The free, incoming fluorophore-labeled alkylthiols replace unlabeled alkylthiols at the surface of the MPCs. When bound to the nanoparticles, the fluorescence of the fluorophores is quenched to a certain extent. Interestingly, there is no observable change in the position or shape of the emission spectra, even for the highly solvatochromic DABP and DANS chromophores. This indicates that the chromophore remains principally surrounded by solvent molecules when bound to the MPC.

The equilibration is monitored by fluorescence spectroscopy. When varying the relative amounts of incoming thiolalkylated fluorophores (defined as β, see Section 2), it is observed that the final relative fluorescence intensities (I/I_0) at equilibrium are different (see Figure 3). The kinetics of exchange seem to follow the second-order Langmuir kinetics observed recently by Kassam et al. for the exchange between alkylthiols of different chain lengths of gold MPCs.[43] For our analysis we are mainly interested in the final equilibrium intensity. The kinetics serve to confirm completion of the equilibration process.

Additionally, we verified for all three fluorophores that the fluorescence of fluorophore without alkylthiol function (Figure 4) did not change in the presence of gold MPCs. Indeed, without the alkylthiol arm, the fluorescence intensities of the fluorophores remained at their initial levels over time (e.g., see Figure 3, open squares for DABP), indicating that (1) there is no "nonspecific" binding of the chromophore to the MPCs and (2) there is no intermolecular quenching of the fluorescence by MPCs at the concentrations used. For quenching of fluorescent singlet excited states by a diffusion-controlled collisional process much higher concentrations of quencher ($> 10^{-3}$ M) are needed than employed in the present study ($< 10^{-7}$ M in MPCs). Thus, the gradual decrease of the fluorescence in the case of thiolalkylated pyr-C11SH, DANS-C11SH, and DABP-C11SH is only caused by their insertion into the monolayer at the surface of the gold MPCs. After completion of the fluorescence measurements on the equilibrated mixtures, it was observed that the initial fluorescence intensitiy of each solution could be recovered by addition of an excess of *n*-dodecanethiol (10^{-2} M) to liberate the bound chromophores from the particle surface (see Supporting Information). This observation demonstrates the reversibility of the binding.

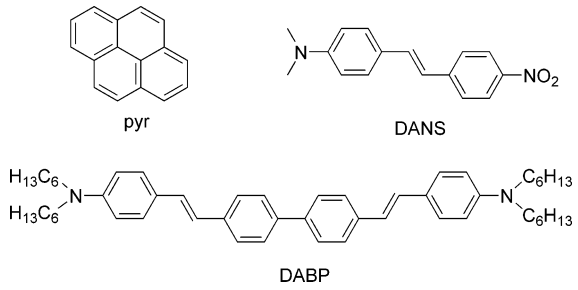

Figure 4. Structures of the unmodified chromophores used as reference compounds. There are small differences in the alkyl chains used on the aniline moieties compared to the thiol-modified chromophores. Pyrene and DANS are commercially available. DABP has been described in ref 42.

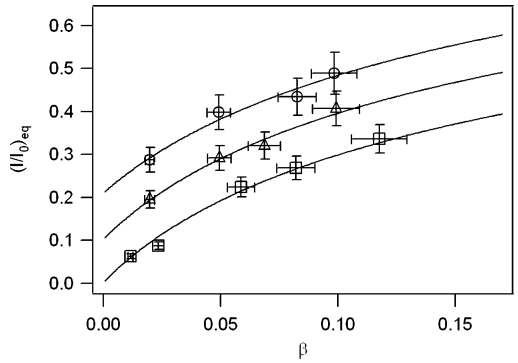

Figure 5. Relative fluorescence intensities $(I/I_0)_{eq}$ at equilibrium of pyr-C11SH (open squares), DANS-C11SH (triangles), and DABP-C11SH (circles) added in different concentrations relative to the number of MPC binding sites (β). The solid lines are fits of eq 14 to the data using the parameters listed in Table 1.

The amount of incoming fluorescent thiol was varied from approximately $\beta = 0.01-0.1$ (1−10% with respect to the number of available binding sites) for all three fluorophores, pyr-C11SH, DANS-C11SH, and DABP-C11SH. The kinetics were followed, and the final relative fluorescence intensity at equilibrium, $(I_0/I)_{eq}$ was determined for each sample, resulting in the set of data represented in Figure 5. The amount of incoming fluorescent thiol was deliberately kept low in this study to avoid interactions between chromophores once bound to the metal nanoparticle.

The titration curves in Figure 5 can be successfully analyzed in terms of the simple dynamic-equilibrium model (Section 2). The solid lines are fits of eq 14 to the data using two parameters: K, the equilibrium constant, and Q, the relative fluorescence brightness, of a bound chromophore compared to a free chromophore. The combinations of K and Q obtained for each fluorescent thiol/MPC pair are collected in Table 1.

When considering the obtained equilibrium constants K, it is seen that their values clearly deviate from 1. In contrast to

Table 1. Equilibrium Constant *K* and Relative Brightness, *Q*, for the Three Thiol-modified Chromophores in the Ligand Exchange on 4.5 nm Diameter Gold MPCs, Obtained through Fits of Eq 14 to the Data in Figure 5

	K	*Q*
pyr-C11SH	0.18[a]	0.003 ± 0.005
DANS-C11SH	0.18 ± 0.04	0.10 ± 0.03
DABP-C11SH	0.21 ± 0.06	0.21 ± 0.04

[a] For pyr-C11SH, *K* was kept fixed at 0.18 for fitting since an unconstrained fit yields a slightly negative *Q* ($K = 0.16 \pm 0.02$, $Q = -0.01 \pm 0.02$). From both the constrained and unconstrained fits it can be concluded that the relative brightness of pyr-C11SH bound to the particles is very low.

experiments on the exchange of *n*-alkylthiols of different chain lengths on gold MPCs,[43] in which it was found that $K \approx 1$, we find in this study $K \approx 0.2$ for exchange using fluorophore-modified alkylthiols. This reduced affinity of the modified alkylthiols can be understood considering the differences in chemical structure of the simple *n*-dodecanethiols and their fluorophore-modified counterparts, which apparently make it more difficult to insert these modified thiols into pristine monolayers of *n*-dodecanethiol.

Our results demonstrate that one cannot assume that $K \approx 1$ in all cases. The simple equilibrium model used here, however, provides a way of measuring *K* and subsequently using this knowledge to optimize the experimental conditions to arrive at the desired loading of the monolayer. Once *K* is known, the equilibrium distribution of free and bound chromophore for any given β can be calculated.

In addition to *K*, the fits of eq 14 to the data yield the relative fluorescence brightness of a nanoparticle-bound fluorophore, *Q*, for each of the fluorophores studied. The relative brightness is proportional to the product of the fluorescence quantum yield (Φ) and the extinction coefficient at the excitation wavelength (ϵ). In all three cases the brightness is reduced compared to the free fluorophores but not by the same amount for each of the fluorophores. Table 2 lists photophysical data for the three fluorophore-modified alkylthiols (free in toluene solution), as well as the absolute brightness of the bound fluorophores, calculated using these data and *Q*.

It was noted that the fluorescence quantum yield of DABP-C11SH and DANS-C11SH differs from the quantum yield of the unmodified chromophores. From this observation, we conclude that the introduction of the alkylthiol chain leads to the introduction of a fluorescence quenching pathway in DABP-C11SH. It is likely that this quenching is mediated by the thiol group. In this case it may be desirable to compare the brightness of the bound dye-C11SH directly to the brightness of the *unmodified* chromophore (i.e., not carrying the alkylthiol moiety), according to eq 18, since it might be expected that the thiol group loses its quenching ability once it is bound to the gold surface.

$$Q' = \frac{(\epsilon\Phi)_{\mathrm{Fb}}}{(\epsilon\Phi)_{\mathrm{fluorophore}}} \tag{18}$$

Table 3 lists the photophysical data and the "corrected" relative brightness, Q', for a fluorophore on the MPC surface compared to the free, non-thiol-modified parent chromophore. The corrected brightness, Q', follows the same trend as the relative brightness, *Q*, with the quenching effect of the MPCs appearing more pronounced. Since the photoluminescence brightness is the product of the extinction coefficient and the fluorescence quantum yield, changes in Q' may be due to changes in extinction coefficient (ϵ) and/or changes in fluorescence quantum yield (Φ). A change in extinction coefficient induced by the metal nanocore cannot be excluded beforehand, and it is thus interesting to study the effect of binding of the chromophore to the gold MPCs on the UV−vis absorption spectra.

Table 2. Optical Absorption and Emission Data for the Free Thiol-Modified Dyes 1, 2, and 3, as Well as the Absolute Brightness ($\epsilon\Phi$) of Free (F_f) and Bound (F_b) Dye[a]

	$\lambda_{\mathrm{abs,max}}$ nm	ϵ_{Ff}[b] $M^{-1}\,cm^{-1}$	Φ_{Ff}[c]	$(\epsilon\Phi)_{\mathrm{Ff}}$[d] $M^{-1}\,cm^{-1}$	$(\epsilon\Phi)_{\mathrm{Fb}}$[e] $M^{-1}\,cm^{-1}$
pyr-C11SH	346	3.4×10^4	0.10	3.4×10^3	0
DANS-C11SH	432	3.2×10^4	0.60	1.9×10^4	1.9×10^3
DABP-C11SH	399	8.4×10^4	0.47	3.9×10^4	8.3×10^3

[a] All measurements were in air-equilibrated toluene. [b] Extinction coefficient of the free alkylthiol-modified fluorophore. [c] Fluorescence quantum yield of the free alkylthiol-modified fluorophore. [d] Fluorescence brightness of the free fluorophore. [e] Fluorescence brightness of the bound fluorophore.

Table 3. Absorption and Emission Data for the Unmodified Parent Chromophores, and the Calculated Relative Brightness, Q', of a Bound Dye Compared to the Non-Thiol-Modified Dye[a]

	ϵ_{max} $M^{-1}\,cm^{-1}$	F	$(\epsilon\Phi)^{\mathrm{flphore}}$ $M^{-1}\,cm^{-1}$	Q'
pyrene	3.7×104	0.03	1.1×103	0
DANS	2.9×104	0.79	2.3×104	0.083
DABP	8.3×104	0.77	6.4×104	0.13

[a] All measurements were in air-equilibrated toluene.

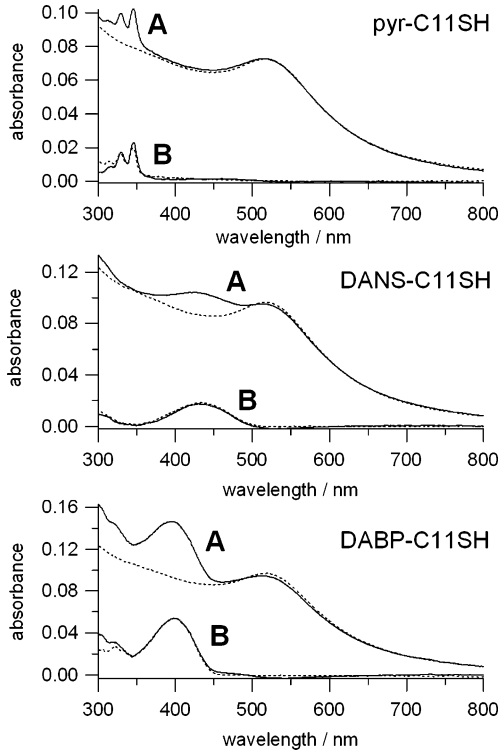

Figure 6. Effect of gold MPCs on the UV−vis absorption of bound chromophores. The dye concentration was at 10% of the number of thiol binding sites ($\beta = 0.1$). "A", solid lines: UV−vis spectra of solutions of alkylthiol-modified dyes and gold MPCs in toluene, after equilibration. "A", dotted lines: UV−vis spectra of MPCs alone in toluene. "B", solid lines: spectra of alkylthiol-modified dyes and gold MPCs in toluene after subtraction of the MPC absorption spectrum. "B", dotted lines: absorption spectra of alkylthiol-modified dye alone in toluene, for comparison.

UV−vis spectra of equilibrated mixtures of 4.5 nm gold MPCs and dye-C11SH (10% relative to the number of binding sites, $\beta = 0.1$, Figure 6) provide useful information on the behavior of the extinction coefficients of the dyes upon binding to the

gold nanoparticles. After subtraction of the absorption bands related to the gold MPC core, the remaining dye absorption spectra show no observable change compared to the absorption spectra of the free dye-C11SH compounds. With $K = 0.2$ and $\beta = 0.1$, one can estimate that in these equilibrated samples 28% of the dye-C11SH are free in solution and 72% are bound to a nanoparticle. With such an amount of bound chromophores contributing to the absorption spectra, even relatively minor changes in the absorption spectrum of the dyes upon binding to the nanoparticles would have been clearly identifiable. The data show that the 4.5 nm diameter gold nanoparticles have no observable effect of the UV−vis absorption of the attached dyes. The decrease in brightness can therefore be exclusively attributed to a quenching of the fluorescent state by the nanoparticle, without a change in effective extinction coefficient of the chromophore.

The gold nanoparticle-induced decrease in brightness in the present assemblies seems to be caused by enhancement of nonradiative processes leading to a quenching of the fluorescence. In molecular photophysical terms this quenching can be ascribed to electron and/or energy transfer. The most common mechanisms of energy transfer (Förster and Dexter mechanisms)[47] are governed by spectral overlap. However, there is no direct correlation between Q' and the spectral overlap between dye emission and MPC absorption.

A tentative qualitative explanation of the observed trend may be as follows. The gold MPC absorption profile is a sum of the "pure" plasmon resonance at long wavelengths (> ∼450 nm) and d−sp interband transitions at shorter wavelengths. Taking this into account, the excited-state of pyrene may interact mainly with the gold MPC interband transitions, DANS mainly with the plasmon resonance, and DABP falls "in between" these two types of transitions, leading to less fluorescence quenching. The MPCs studied are relatively small, 4.5 nm, compared to other types of gold colloids (e.g., those obtained through citrate reduction which are often >10 nm). The plasmon band in the present MPCs is damped, and the contribution of the interband absorption is relatively important. Additionally, the fluorescence quenching may contain contributions from electron-transfer processes. The generation of radical cations[48] in pyrene-functionalized gold MPCs has been observed using transient-absorption spectroscopy.

An alternative quenching mechanism may be furnished by the theory of Persson and Lang,[49] as implemented recently for very small (1.5 nm diameter) gold nanoparticles and fluorescent dyes, termed NSET for "nanosurface energy transfer".[28] This energy transfer mechanism, which displays a fourth-power distance dependence, does not depend on spectral overlap. Metal nanoparticle size, however, may be a determinant factor for the mode of energy transfer, and differently sized particles may have different mechanisms of fluorescence quenching. More quantitative data on a diverse set of different metal particle−chromophore systems may clarify which theoretical description is most adequate. The fluorimetric method described in this paper may be one of the ways to obtain such quantitative data, especially when combined with time-resolved spectroscopic measurements, that yield information on excited-state lifetimes and on the nature of the states involved in nonradiative relaxation.

5. Conclusions

Using place exchange reactions on the surface of monolayer-protected gold nanoparticles, we have studied the quenching of fluorescent chromophore by the metal core. The present study not only unambiguously confirms that blue, yellow, and green emitting pyrene, DANS, and DABP chromophores are quenched by 4.5 nm diameter gold nanoparticles but also quantifies this decrease in fluorescence brightness. The metal nanoparticle-induced decrease in brightness in these systems amounts to 100%, 92%, and 83% for pyrene, DANS, and DABP, respectively, and appears to stem from effects on the light emission step only, since the absorption spectra of the chromophores are virtually unaffected. The exact mechanism of the fluorescence quenching is not entirely understood, and further studies will be necessary to elucidate, for example, the effect of nanoparticle size on the quenching, as recent studies[11,12,14,25,27,50,51] have involved gold nanoparticles of diameters varying from 1 nm (not displaying a plasmon resonance) to beyond 10 nm (displaying a dominant surface plasmon resonance).

Analysis of the equilibrium of ligand exchange with competing fluorophore-modified and unmodified alkylthiols yields an equilibrium constant clearly inferior to 1 for the insertion of a fluorophore-ester functionalized alkylthiol into a pristine monolayer of *n*-dodecanethiol, indicative of a reduced "solubility" of the functionalized alkylthiol in the monolayer. Fluorescence may be a sensitive and convenient tool for investigating the effect of monolayer composition and dopant structure on place exchange equilibria. In spite of the assumptions made, the simple model for place exchange equilibria presented in this work enables quantitative control of the number of active functions introduced in the monolayer of MPCs.

Acknowledgment. The authors express their sincere thanks to Grégory Schneider (Institut Charles Sadron, Strasbourg) for performing transmission electron microscopy, and Olivier Mongin (CNRS UMR6510, Université de Rennes 1) for synthetic chemical advice and providing hydroxy-modified DANS. N.N. received a doctoral fellowship from the French Ministry of Education and Research.

Supporting Information Available: Synthesis of the hydroxy-terminated DABP derivative, electron micrograph of the nanoparticles, details on the determination of the number of thiol binding sites on the nanoparticle surface, and the liberation of bound fluorophores observed through fluorescence spectroscopy. This material is available free of charge via the Internet at http://pubs.acs.org.

LA070005A

(47) Turro, N. J. *Modern Molecular Photochemistry*; University Science Books: Sausalito CA, 1991.
(48) Ipe, B. I.; Thomas, K. G.; Barazzouk, S.; Hotchandani, S.; Kamat, P. V. *J. Phys. Chem. B* **2002**, *106*, 18−21.
(49) Persson, B. N. J.; Lang, N. D. *Phys. Rev. B* **1982**, *26*, 5409−5415.
(50) Dulkeith, E.; Morteani, A. C.; Niedereichholz, T.; Klar, T. A.; Feldmann, J.; Levi, S. A.; Van Veggel, F. C. J. M.; Reinhoudt, D. N.; Möller, M.; Gittins, D. I. *Phys. Rev. Lett.* **2002**, *89*, 203002.
(51) Thomas, K. G.; Kamat, P. V. *Acc. Chem. Res.* **2003**, *36*, 888−898.